Reversible Self-Association of a Human Myeloma Protein. Thermodynamics and Relevance to Viscosity Effects and Solubility†

Craig G. Hall* and George N. Abraham

ABSTRACT: Monoclonal IgG paraproteins associated with multiple myeloma, Felty's syndrome, and idiopathic cryoglobulinemia frequently produce disease due to a tendency to self-associate in vivo. The insolubility and viscosity effects of these proteins are of specific interest as molecular disease mechanisms. In sedimentation equilibrium studies at 21 °C an IgG1–λ myeloma protein (IgG–MIT) associated with the hyperviscosity syndrome is shown to undergo a reversible polymerization reaction. On the basis of the theory and data-fitting methods of Adams and co-workers [Tang, L. H., Powell, D. R., Escott, B. M., & Adams, E. T., Jr. (1977) *Biophys. Chem. 7*, 121–139], the data are consistent with a nonideal cooperative indefinite (SEK type III) model self-association in which one equilibrium constant (K_{12} = 6.3 × 10^3 L/m) governs dimerization while another (K = 1.7 × 10^4 L/m) governs all subsequent additions of monomer to the polymer. Temperature effects on K_{12} and K between 11 and 30 °C suggest negative van't Hoff enthalpies for all association steps and a positive entropy change [$\Delta S°$ = 2.5 cal/(mol-deg)] for steps beyond the dimer. An increase in ionic strength from I = 0.03 to I = 0.18 promotes the polymerization of IgG–MIT through a marked increase in K while paradoxically enhancing bulk solubility. These results suggest that this self-association proceeds through a combination of weak nonionic and hydrophobic interactions. The enhancement of both polymerization and solubility by increased ionic strength suggests that the hyperviscosity induced by IgG–MIT results from its ability to form large, highly soluble polymers in serum. A theory is advanced to explain the previously observed coincidence of hyperviscosity effects and euglobulin solubility behavior of IgG paraproteins.

Many proteins undergo reversible self-association reactions in aqueous solution, and examples of spontaneous protein associations are important in both normal and pathologic molecular processes. The polymerizations of viral coat proteins (Lauffer, 1975), actin (Oosawa & Kasai, 1971), spectrin (Ungewickell & Gratzer, 1978), tubulin (Olmsted & Borisy, 1973), and flagellin (Asakura, 1968) contribute to the formation and stability of normal subcellular structures. The self-associations of pyruvate dehydrogenase (Vogel et al., 1972) and pyruvate carboxylase (Lowenstein, 1967) appear to influence enzymatic activity and functional regulation. For the bovine β-lactoglobulins (Tang et al., 1977; Sarquis & Adams, 1977), insulin (Jeffrey & Coates, 1966), and ACTH (Squire & Li, 1961), self-association, though well-known, is of unclear significance.

Monoclonal serum immunoglobulins found in various lymphoproliferative disorders may self-associate and thus contribute to the pathophysiology of idiopathic cryoglobulinemia (Brouet et al., 1975) and the hyperviscosity syndromes of rheumatoid arthritis (Pope et al., 1975), multiple myeloma (Bjorneboe & Jensen, 1966; Kochwa et al., 1966; Lindsley et al., 1973), and other plasma cell and lymphocytic dyscrasias (Kyle & Bayrd, 1976). The tendency of monoclonal immunoglobulins and their constituent chains to self-associate may contribute to the assembly of immunoglobulin molecules in vivo (Green, 1973; Stevens et al., 1980). Due to their unique structural polymorphism, the monoclonal immunoglobulins provide a model system for study of the structural bases of protein–protein interactions and protein solubility phenomena.

The ability of a protein to polymerize in solution bears heavily upon its thermodynamic activity, hence solubility. Previous studies (Scoville et al., 1979, 1980; Middaugh et al., 1978; Vialtel et al., 1982) concerning the precipitation kinetics of monoclonal cryoimmunoglobulins have demonstrated the importance of an intermolecular nucleation event in cryoprecipitation. Other studies have suggested that immunoglobulin self-association may involve ionic interactions (Kochwa et al., 1966; Green, 1973; Vialtel et al., 1982; Klein et al., 1977; Middaugh & Litman, 1977a,b), dispersion forces (Middaugh & Litman, 1977a,b; Middaugh et al., 1980) and hydrophobic interactions (Parker & Osterland, 1970; Erikson et al., 1982).

While these interactions must have their bases in certain features of protein structure, no unifying molecular concept for self-association of monoclonal immunoglobulins has emerged. Attempts to relate primary sequence data to self-association have consisted in identifying unique amino acid substitutions in the variable region domains (Erikson et al., 1982). The significance of these findings remains unclear. A detailed knowledge of the physical nature and structural location of the molecular interactions involved in self-association of monoclonal immunoglobulins should help clarify the role of primary structural features in the polymerization process.

This report presents the results of equilibrium sedimentation studies on the reversible, concentration-dependent self-association of a cold-soluble IgG1–λ myeloma protein (IgG–MIT) isolated from a patient with multiple myeloma, serum hyperviscosity, and the hyperviscosity syndrome. On the basis of the theory and data analysis methods of Adams (Adams et al., 1978; Chun et al., 1972; Tang et al., 1977), apparent molecular weight data for IgG–MIT were consistent with a cooperative indefinite self-association. The effects of ionic strength and temperature suggest that the association is mediated by dispersion forces and hydrophobic interactions. The

† From the Department of Microbiology (C.G.H. and G.N.A.) and the Department of Medicine and Division of Immunology (G.N.A.), University of Rochester School of Medicine, Rochester, New York 14642. *Received November 30, 1983; revised manuscript received May 1, 1984.* This work was supported in part by U.S. Public Health Service Grants AI-19658 and AI-21288, U.S. Public Health Service Training Grant AI-00028, The James P. Wilmot Foundation, the David Welk Memorial Fund, and National Institutes of Health Medical Scientist Training Grant GM-07356. This work represents partial fulfillment of the research requirements for the Ph.D. degree in microbiology for C.G.H., a trainee in the NIH Medical Scientist Training Program.

0006-2960/84/0423-5123$01.50/0

enhancement of both polymerization and bulk solubility of IgG–MIT by increasing ionic strength in the physiologic range suggests a molecular mechanism for hyperviscosity effects which is distinct from the nucleation-controlled precipitation process of some monoclonal cryoimmunoglobulins. The findings also point up certain pitfalls in the use of nonequilibrium methods to detect protein interactions and in the use of cosolvent methods [poly(ethylene glycol) precipitation] to study protein solubility.

Materials and Methods

Protein Isolation. IgG–MIT was present in plasma samples at roughly 7 g % and remained soluble in plasma at 4 °C. IgG was isolated by precipitation with 16% Na_2SO_4. The precipitate was redissolved in 0.15 M phosphate buffer (pH 7.4), dialyzed against 0.015 M phosphate buffer (pH 7.4), and chromatographed at 37 °C over DEAE-cellulose equilibrated with the latter buffer. The column eluate, incubated at 4 °C, yielded a clear gelatinous precipitate. After several reprecipitations from 0.015 M phosphate buffer (pH 7.4), the precipitated protein produced a single band on sodium dodecyl sulfate (SDS)–polyacrylamide gel electrophoresis and contained only an IgG–λ paraprotein in immunodiffusion and immunoelectrophoresis developed with antisera specific for immunoglobulin heavy chain and light chain types. In previous studies, the IgG–MIT paraprotein isolated in this way revealed a restricted isoelectric focusing profile typical of monoclonal immunoglobulin (pI = 7.3) and single N-terminal amino acid sequences for both heavy and light chains (Abraham et al., 1979).

Sedimentation Studies. A Beckman Model E analytical ultracentrifuge equipped with schlieren and Rayleigh interference optics and RTIC thermostat system was employed. Protein samples were dialyzed against phosphate buffer (pH 7.4), and the dialysate served as an optical blank in each experiment. Short column equilibrium runs were made by using a 12-mm capillary-type synthetic boundary cell which permitted a subsequent determination of the initial solute concentration (Klainer & Kegeles, 1955). An inert fluorocarbon oil was used as a bottom fluid in each experiment. Optical patterns were recorded on Kodak metallographic plates and analyzed on a digital microcomparator. Apparent z-average molecular weights were calculated by the combined optics method using the equation (Chervenka, 1969)

$$M_{za} = \frac{RT}{(1 - \phi'\rho)\omega^2} \frac{d}{dc}\left[\frac{1}{r}\frac{dc}{dr}\right] \quad (1)$$

Here R is the gas constant, T is the absolute temperature, ϕ' is the solute partial specific volume, ρ is the solution density, ω is the angular velocity, r is the radial distance, and c is the solute concentration. Apparent weight-average molecular weights were obtained from interference optical data by using the relation (Chervenka, 1969)

$$M_{wa} = \frac{2RT}{(1 - \phi'\rho)\omega^2}\left[\frac{d \ln c}{dr^2}\right] \quad (2)$$

Apparent molecular weights at low solute concentrations were determined by the Yphantis meniscus depletion method with appropriate corrections for fringe nonlinearity (Yphantis, 1964). Sedimentation velocity runs were made at 56 000 rpm by using an aluminum (An-D) rotor with 12-mm double sector cells and schlieren optics.

Auxiliary Measurements. Buffer densities and partial specific volume for IgG–MIT were determined pycnometrically at 25 °C (ϕ'_{MIT} = 0.742 cm^3/g). Sample solution densities were estimated by using the relation (Chevenka, 1969)

$$\rho_{solution} = \rho_{solvent} = c(1 - \rho_{solvent}\,\phi'_{solute}) \quad (3)$$

where c is protein concentration in grams per milliliter. Temperature corrections for ϕ' were made by using a temperature coefficient of 4 × 10^{-4} cm^3/deg (Bull & Breese, 1968). All synthetic boundary determinations of initial solute concentration were made at 21 °C and corrected to the appropriate temperature (Adams & Filmer, 1966). An extinction coefficient at 280 nm of ϵ^1_{1cm} = 14.6, determined by micro-Kjeldahl analysis (Scoville et al., 1979), was used in optical calibration of the Model E yielding 4.56 fringes mg^{-1} mL^{-1} for IgG–MIT at 21 °C. This value was also temperature corrected where appropriate (Adams & Filmer, 1966).

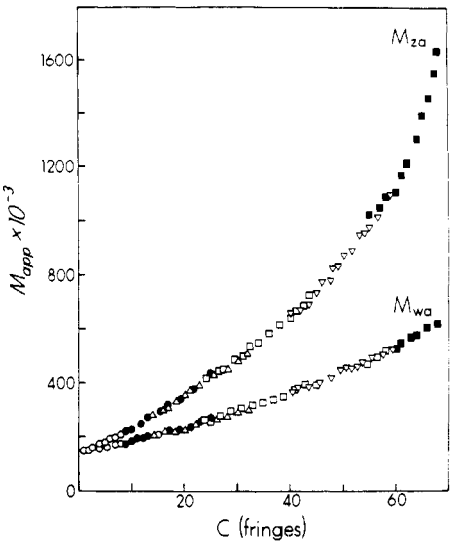

FIGURE 1: Concentration dependence of M_{za} and M_{wa} for IgG–MIT at 21 °C in 0.015 M phosphate buffer, pH 7.4 (I = 0.03). Various symbols represent results from experiments at different initial protein concentrations.

Results

Apparent z-average (M_{za}) and apparent weight-average (M_{wa}) molecular weights for IgG–MIT at 21 °C were computed as described from schlieren and Rayleigh optical data, respectively. Their concentration dependencies are shown in Figure 1. These apparent average molecular weight curves converge at infinite dilution upon the true monomer molecular weight, M_1 (~147 000). Three lines of evidence indicate that the observed molecular weight heterogeneity, evident in the inequality of M_{za} and M_{wa} at all concentrations, is due to reversible self-association rather than to the presence of stable aggregates. First, under sedimentation transport conditions only a single (7S) boundary was observed by schlieren optics. Second, IgG–MIT samples ultrafiltered through a M_r 300 000 cutoff membrane prior to equilibrium centrifugation showed no loss of optical density and gave apparent molecular weight data that were quantitively identical with those obtained for unfiltered samples. Third, as shown in Figure 1, data from several equilibrium runs at different initial protein concentrations fell on a continuous curve. M_{za} or M_{wa} values obtained at the same fringe count in different experiments were similar.

The theory of Adams (Adams et al., 1978; Chun et al., 1972; Tang et al., 1977) was employed to fit the data to an equilibrium self-association model. Three assumptions regarding the associating species are central to this approach (Chun et al., 1972): (1) the apparent specific volumes (ϕ') are equal, (2) the refractive index increments $[(\partial n/\partial c)_{T,\mu}]$ are equal, and

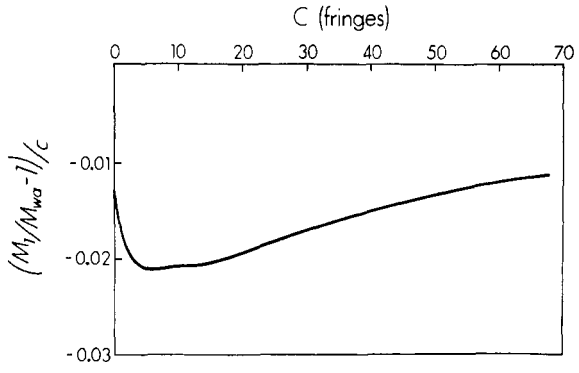

FIGURE 2: Plot of $[(M_1/M_{wa}) - 1]/C$ vs. C based on experimental data shown in Figure 1. The area bounded by the curve and the abscissa is computed to assess $\ln f_a$ at each C.

(3) the activity coefficient (y_i) for each species is described by

$$\ln y_i = iBM_1C \qquad (i = 2, 3, \ldots) \tag{4}$$

where BM_1 is the second virial coefficient, M_1 is the monomer molecular weight, and C is the total solute concentration (mg/mL). These assumptions permit analysis of the expermental data to test for the type of association present and to determine values for association constants (K_i) and the nonideal term (BM_1). B is a constant whose value depends on temperature and solute–solvent combination ($B = 0$ in an ideal solution), providing a concentration-dependent correction for apparent molecular weights obtained under nonideal conditions.

The analysis is based upon knowledge of three quantities as functions of concentration, M_1/M_{wa}, M_1/M_{na} (where M_{na} is the apparent number-average molecular weight), and $\ln f_a$ (where f_a is the apparent weight fraction of monomer). M_1/M_{wa} and M_1/M_{na} were computed from a smoothed curve of M_{wa} vs. C, the latter by numerical integration using the trapezoidal rule and the relation (Adams et al., 1978)

$$\frac{1}{M_{na}} = \frac{1}{C}\int_0^C \frac{1}{M_{wa}}\,dC \tag{5}$$

M_{wa} is similarly related to M_{za} (Klainer & Kegeles, 1955):

$$\frac{1}{M_{na}} = \frac{1}{C}\int_0^C M_{za}\,dC \tag{6}$$

The quantity $\ln f_a$ was obtained by using the relation (Adams et al., 1978)

$$\ln f_a = \int_0^C \left(\frac{M_1}{M_{wa}} - 1\right)\frac{dC}{C} \tag{7}$$

Numerical integration by the trapezoidal rule of a plot of $(1/C)(M_1/M_{wa} - 1)$ vs. C (Figure 2) thus yields a value for $\ln f_a$ at each concentration. All three fractional quantities derived from the experimental data are plotted in Figure 3.

The apparent quantities M_1/M_{wa}, M_1/M_{na}, and f_a measured under nonideal conditions are related to their true counterparts M_1/M_{wc}, M_1/M_{nc}, and f_1 by the nonideal term BM_1 (Adams et al., 1978):

$$\frac{M_1}{M_{wa}} = \frac{M_1}{M_{wc}} + BM_1C \tag{8}$$

$$\frac{M_1}{M_{na}} = \frac{M_1}{M_{nc}} + \frac{BM_1C}{2} \tag{9}$$

$$\ln f_a = \ln f_1 + BM_1C \tag{10}$$

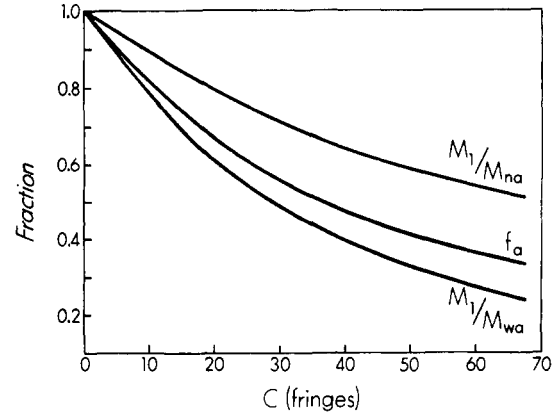

FIGURE 3: Plot of fractional quantities required for the Adams analysis of protein self-association for IgG–MIT, based on data in Figure 1. Curves were derived as described in the text by using M_1 147 000.

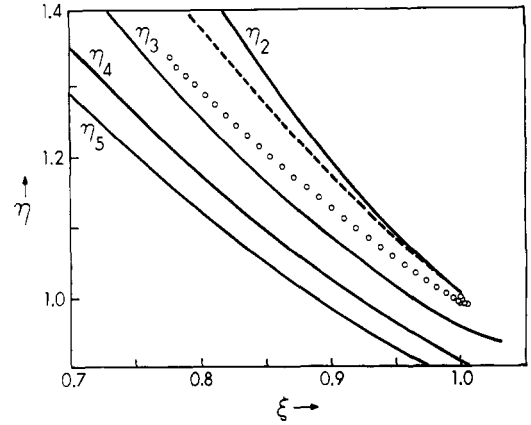

FIGURE 4: Plot of the quantities η vs. ξ for self-association of IgG–MIT at 21 °C, $I = 0.03$, derived from experimental data is represented by (O). For comparison, standard plots based on published equations (Chun et al., 1972) are included. Lines labeled η_n represent η for various discrete monomer–n-mer model associations. (---) represents η_{ind} for the SEK type I model (indefinite isodesmic) association.

Chun et al. (1972) have shown that these equations can be combined to eliminate the nonideal term, yielding two useful diagnostic functions:

$$\xi = \frac{2M_1}{M_{na}} - \frac{M_1}{M_{wa}} = \frac{2M_1}{M_{nc}} - \frac{M_1}{M_{wc}} \tag{11}$$

$$\eta = \frac{M_1}{M_{wa}} - \ln f_a = \frac{M_1}{M_{wc}} - \ln f_1 \tag{12}$$

A plot of η vs. ξ based on the data for IgG–MIT at 21 °C is shown in Figure 4. Theoretical curves are included for various discrete (monomer–n-mer) model associations and for one unlimited model (the SEK type I, or isodesmic) association, based on equations given by Chun et al. (1972). Clearly, none of these models adequately describes the data for IgG–MIT. However, the steadily increasing values of M_{wa} at high concentrations and the tendency of IgG–MIT to precipitate seemed to suggest an unlimited association.

In the SEK type I model unlimited association, it is assumed that (i) $\Delta G°$, the free energy of association (hence, K), for each polymerization step is the same and (ii) the total solute concentration may be expressed as an infinite series which converges for values of $KC_1 < 1$ (where C_1 is the monomer concentration) (Adams et al., 1978). More complex indefinite association models arise when assumption i is relaxed, allowing the K's for various steps to differ. Inspection of two further diagnostic data plots gave direction in choosing a model. For

Table I: Fit Parameters for the Self-Association of IgG–MIT at 21 °C in 0.015 M Phosphate Buffers, pH 7.4

SEK model	$BM \times 10^3$ (L/g)[a]	$BM_1 \times 10^3$ (L/g)[b]	$k_{12} \times 10^{-3}$ (M^{-1})	$k \times 10^{-4}$ (M^{-1})	$(1/n)\cdot\sum(\delta_i)^2$
			$I = 0.03$		
II	3.93 ± 6.06	−8.66	N/A	1.68	7.10×10^{-4}
III	−4.23 ± 2.37	−5.88	6.50	1.59	4.28×10^{-6}
IV	3.93 ± 6.06	−4.01	11.70	3.05	1.07×10^{-4}
			$I = 0.18$		
III	−8.25 ± 1.73	−8.66	2.95	1.82	3.50×10^{-6}

[a] Average pointwise value ± standard deviation; $C^* = 12$ fringes for $I = 0.03$; $C^* = 18$ fringes for $I = 0.18$; values determined iteratively by method II of Tang (Tang et al., 1977). [b] Best-fit BM_1 values obtained by floating all parameters. Note that only for the SEK type III fit does the best-fit value fall within the range of values generated explicitly by using the iterative method (Tang et al., 1977).

Table II: Fit Parameters for Self-Association of IgG–MIT in 0.015 M Phosphate Buffer, pH 7.4 ($I = 0.03$), at Three Temperatures

SEK model	temp (°C)	$BM_1 \times 10^3$ (L/g)[a]	$BM_1 \times 10^3$ (L/g)[b]	$k_{12} \times 10^{-3}$ (M^{-1})	$k \times 10^{-3}$ (M^{-1})	$(1/n)\cdot\sum(\delta_i)^2$
III	11	−9.38 ± 0.776	−9.81	10.60	2.11	9.04×10^{-6}
III	21	−4.23 ± 2.37	−5.88	6.50	1.59	4.28×10^{-6}
III	30	−6.59 ± 2.05	−6.61	3.68	1.22	8.47×10^{-6}

[a] Average pointwise value ± standard deviation as determined iteratively by method II of Tang (Tang et al., 1977). C^* was 12 fringes for 11 °C data, 12 fringes for 21 °C data, and 22 fringes for 30 °C data. [b] Best-fit BM_1 value obtained by floating parameters.

a system obeying the SEK type I unlimited association model, ξ is quadratic in $f_1^{1/2}$ (Chun et al., 1972). Thus, f_1 can be calculated from the experimental data and a plot of $1 - f_1^{1/2}$ vs. Cf_1 should be linear with slope = K, intersecting the origin (Adams et al., 1978; Chun et al., 1972). On the basis of the data for IgG–MIT, this plot was biphasic, suggesting that more than one K was needed to achieve a fit. Reasoning similarly, a plot of

$$\frac{M_1}{M_{wa}} - \frac{f_1^{1/2}}{2 - f_1^{1/2}} = BM_1C \qquad (13)$$

for a system obeying the SEK type I model should be linear with slope BM_1 (Adams et al., 1978; Chun et al., 1972). On the basis of the data for IgG–MIT, this plot was also biphasic with a small negative slope.

An attempt was therefore made to fit the data to an SEK type III unlimited association model (a cooperative variant of the SEK type I) in which one constant (K_{12}) applies to dimerization and another (K) to all subsequent steps (Adams et al., 1978). Since an estimate of BM_1 was in hand, an iterative procedure based on the equation (Tang et al., 1977)

$$\ln \frac{f_a}{f_{a^\bullet}} = \int_{C_\bullet}^{C} \left(\frac{M_1}{M_{wa}} - 1 \right) \frac{dC}{C} = \ln \frac{f_1}{f_{1^\bullet}} + BM_1(C - C_\bullet) \qquad (14)$$

(where $C_\bullet$ is a somewhat arbitrarily chosen low concentration) was employed to generate a best-fit value for BM_1 at each concentration. Values for K_{12} and K were then generated and used with BM_1 to regenerate the original M_{wa} vs. C curve. The criterion for a best fit was that the quantity $\sum(S_i)^2$ be minimized (Tang et al., 1977), where

$$S_i = \left[\left(\frac{M_1}{M_{wa}} \right)_{calcd} - \left(\frac{M_1}{M_{wa}} \right)_{obsd} \right] \qquad (15)$$

Attempts were also made to fit the data to the SEK type II unlimited model and to its cooperative variant the SEK type IV, which resemble the type I and type III models, respectively, except that all odd-numbered species beyond the monomer are absent. Details of these procedures are given by Tang et al. (1977). The results, summarized in Table I, show that the data for IgG–MIT are most consistent with an SEK type III model unlimited self-association.

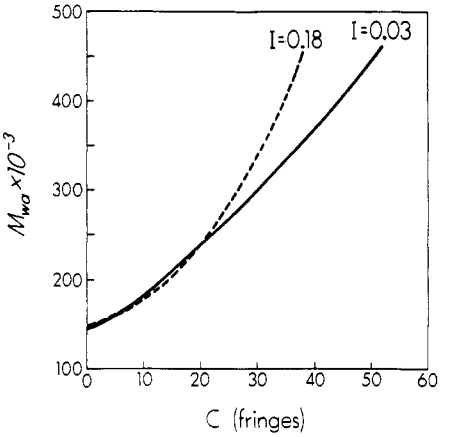

FIGURE 5: Ionic strength effect on M_{wa} vs. C data for IgG–MIT at 21 °C in 0.015 M phosphate buffers, pH 7.4. Buffer with $I = 0.18$ prepared by addition of 0.15 M NaCl. Both plots represent smoothed experimental data from multiple experiments.

Ionic Strength Effects. M_{wa} vs. C data obtained for IgG–MIT in 0.015 M phosphate-buffered 0.15 M NaCl, pH 7.4 ($I = 0.18$), are shown in Figure 5. Raising the ionic strength from $I = 0.03$ to $I = 0.18$ led to a marked increase in M_{wa} at concentrations above 18 fringes (4 mg/mL) while at lower concentrations M_{wa} values were unchanged or slightly decreased. These data also best fit the SEK type III model association with the parameters given in Table I. Remarkably, the enhancement of self-association at higher ionic strength was accompanied by roughly a 5-fold increase in the bulk solubility of IgG–MIT, as judged by concentration thresholds for gel precipitate formation at 4 °C.

van't Hoff Enthalpy and Entropy. M_{wa} vs. C data obtained for IgG–MIT at 11, 21, and 30 °C in 0.015M phosphate buffer, pH 7.4 ($I = 0.03$), are shown in Figure 6. Again, the SEK type III model gave the best data fit at 11 and 30 °C. The results are summarized in Table II. A van't Hoff plot (Figure 7) employing the values for K_{12} and K obtained at 11, 21, and 30 °C yielded the values for $\Delta H°_{12}$, $\Delta S°_{12}$, $\Delta H°$, and $\Delta S°$. The thermodynamic parameters are summarized in Table III.

Discussion

Polymerization of monoclonal immunoglobulins contributes to the pathophysiology of idiopathic cryoglobulinemia (Brouet

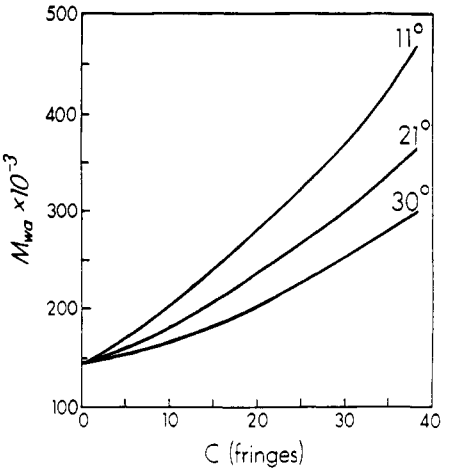

FIGURE 6: Temperature effects on M_{wa} vs. C data for IgG–MIT in 0.015 M phosphate buffer, pH 7.4 (I = 0.03). Curves represent smoothed experimental data from multiple experiments.

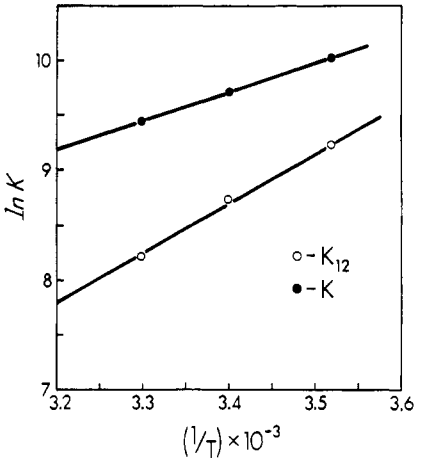

FIGURE 7: van't Hoff plot of ln K vs. $1/T$, where K is the molar association constant and T is the kelvin temperature, based on values of K_{12} and K for IgG–MIT obtained from data in Figure 6 according to the Adams analysis. Plot slope, obtained by linear regression, is $-\Delta H^\circ/R$.

Table III: Thermodynamic Parameters for Self-Association of IgG–MIT in 0.015 M Phosphate Buffer, pH 7.4 (I = 0.03)

T (°C)	ΔG° (kcal/mol)	$T\Delta S^\circ$ (kcal/mol)	ΔS° [cal/(mol-deg)]
	K_{12} (Dimerization)[a]		
11	−5.24	−4.27	−15.0
21	−5.14	−4.37	−14.0
30	−4.95	−4.56	−15.0
	K (Subsequent Steps)[b]		
11	−5.63	0.70	2.5
21	−5.66	0.73	2.5
30	−5.68	0.75	2.5

[a] Based on van't Hoff enthalpy (ΔH°_{12}) = −9.51 kcal/mol. [b] Based on van't Hoff enthalpy (ΔH°) = −4.94 kcal/mol.

et al., 1975) and the hyperviscosity syndrome (Bjorneboe & Jensen, 1966; Kochwa et al., 1966; Lindsley et al., 1973; Kyle & Bayrd, 1976), but the association process and its structural bases remain poorly understood. The application of turbidometric methods to the precipitation of IgG cryoglobulins (Scoville et al., 1979, 1980; Vialtel et al., 1982) has led to a deeper understanding of the kinetics of immunoglobulin self-association. However, rigorous thermodynamic methods have not yet been applied to this clinically important process. Thermodynamic studies should shed light upon the types of interactions mediating self-association and thereby aid in comparative structural analyses of these molecules.

As summarized in Tables I and II, the M_{wa} vs. C data obtained for IgG–MIT under all conditions were best described by a cooperative indefinite (SEK type III) self-association model in which one equilibrium constant (K_{12}) governs dimerization and another (K) governs all subsequent polymerization steps. Attempts to fit the data to an isodesmic association model (SEK type I or II) involving a single equilibrium constant failed. The local minimum in the plot in Figure 2 is also consistent with a model process in which $K_{12} < K$ (Tang et al., 1977; Millthorpe et al., 1975). The values obtained for BM_1 were negative, suggesting an energetic preference for solute association over solute–solvent interactions.

The equilibrium constants obtained from this data analysis suggest weak protein–protein interactions, probably involving some combination of dispersion forces, hydrogen bonding, and/or hydrophobic interactions. The enhancement of self-association of IgG–MIT with increased ionic strength (Figure 5) could be attributed to a shielding of local repulsive charge effects by the supporting electrolyte (NaCl). However, the nonnegative van't Hoff entropy (ΔS°) obtained for polymerization steps beyond the dimer suggests a possible role for hydrophobic interactions. While ionic bond formation may be associated with positive entropy changes (Timasheff, 1973), such an interpretation would clearly be inconsistent with the observed effect of ionic strength on polymerization of IgG–MIT.

In a reaction involving solute association, an nonnegative ΔS° term may suggest the coalescence of nonpolar groups with a consequent increase in the entropy of water. At physiologic temperatures, however, the negative enthalpy of association for IgG–MIT is the more important determinant of free energy and, in view of the salt effect, probably reflects mainly dispersion forces. This contrasts with the entropy-driven polymerizatins of tobacco mosaic virus proteins (Lauffer, 1975; Oosawa & Asakura, 1975; Stevens & Lauffer, 1965; Lauffer & Shalaby, 1980; Shalaby & Lauffer, 1980) for which the enthalpy (ΔH°) of association is nonnegative, the entropy (ΔS°) is highly positive, and the association constant K_a actually increases with temperature in the physiologic range. Since the release of bound water from coalescing nonpolar groups leads to changes in solvation upon polymerization, such systems exhibit both volume increases and substantial heat capacity effects, the latter leading to van't Hoff plot curvature. The linearity of van't Hoff plots for IgG–MIT (Figure 7) and the consistency of experimental values for ϕ' over a range of concentrations (data not shown) support the view that entropy effects are not dominant in this association. Were this not the case, one of the key assumptions of the present analysis (equality of ϕ'_i) might be undermined.

Attempts to draw conclusions about actual molecular events based on the consistency of data with a theoretical model can be hazardous. However, the differential effects of both temperature and ionic strength on the values of K_{12} and K for IgG–MIT support the concept of a two-stage or cooperative process and suggest that the ionic strength effect reflects more than simple electrostatic shielding. A role for hydrophobic interactions is also supported by the more negative nonideal term (BM_1) obtained at the higher ionic strength and by the observation that D_2O promotes the polymerization (data not shown) (Timasheff, 1973).

The concentration-dependent, temperature-dependent and ionic strength dependent polymerization of IgG–MIT suggests a mode of self-association that is distinct from the nucleation-controlled process noted previously for monoclonal IgG

cryoglobulins (Scoville et al., 1979, 1980; Middauch et al., 1978; Vialtel et al., 1982). For IgG–MIT, self-association and precipitation are experimentally separable processes. The ability of IgG–MIT to polymerize extensively yet remain soluble in 150 mM NaCl, while precipitating only at low ionic strength, may explain the presence of hyperviscosity syndrome and the absence of cryoglobulinemia in this patient. Very similar (euglobulin) solubility behavior has been observed to predominate among hyperviscosity-associated IgG paraproteins (Pruzanski & Watt, 1972; Pruzanski & Russell, 1976). Physicochemically, IgG–MIT may thus represent a class of (euglobulin) IgG paraproteins that induce hyperviscosity through formation of large, highly soluble polymers. One might envision such proteins to have discrete hydrophobic and hydrophilic surface regions and to polymerize so as to bury the former and expose the latter to solvent. Studies in progress on the primary structure of IgG–MIT and other IgG paraproteins may permit refinement of this hypothesis.

The observation that increased ionic strength promoted both self-association and bulk solubility of IgG–MIT suggests a direct relationship between polymer size and relative hydrophobicity. Since IgG–MIT polymerizes fairly extensively even at low I, the salt dependence of solubility seems to reflect the physical behavior of the polymer rather than of the monomer; this may have important implications regarding studies of immunoglobulin solubilities. Previous studies of solvent effects (Middaugh et al., 1980; Middaugh & Litman, 1977a,b) and secondary solute effects (Middaugh & Litman, 1977a,b) on the solubilities of monoclonal cryoimmunoglobulins have assumed that solubility changes reflect effects on monomer–monomer interactions. The findings for IgG–MIT suggest that such an assumption may be invalid and that a full understanding of protein solubility processes will require studies of monomer association in solution.

Studies of immunoglobulin solubility using poly(ethylene glycol) (PEG) precipitation (Middaugh et al., 1979, 1980) may also be misleading if applied to polymerizing euglobulins like IgG–MIT. Self-associating proteins are most effectively precipitated by PEG under conditions which favor polymerization (Miekka & Ingham, 1978). However, should polymerization alter the protein surface through sequestration of nonpolar groups, then its effect could be to enhance solubility. In previous studies of monoclonal immunoglobulin solubilities (Middaugh et al., 1979), the linearity of log (solubility) vs. percent of PEG (w/v) plots has been taken to indicate solution ideality (i.e., absence of self-association). However, a pseudolinear plot could obtain for a self-associating protein which appears more hydrophilic in polymerized form such as IgG–MIT. This would lead to an erroneous determination of apparent thermodynamic activity. Such an effect could explain the surprising linearity of semilog plots for hemoglobin S and deoxyhemoglobin A obtained in this system (Middaugh et al., 1979), since both are known to undergo self-association mediated to some extent by hydrophobic interactions (White & Hegan, 1970; Desnica, 1979). Data obtained in this laboratory (to be published) suggest that self-assocdiation below the solubility threshold is common among monoclonal IgGs. Hence, on the basis of the criterion of ideality, few would prove suitable candidates for activity determinations using PEG.

Failure to detect the self-association of IgG–MIT by sedimentation transport methods may be due to disruption of the relatively weak associative interactions by shear forces generated at 56000 rpm (Hall & Abraham, 1984). In previous studies on monoclonal IgGs (Vialtel et al., 1982) and light chains (Kelin et al., 1977) a single schlieren peak during transport was taken as evidence that soluble polymers were not present during subsequent turbidometric or spectroscopic measurements. The findings for IgG–MIT argue that some equilibrium thermodynamic technique must be employed to rule out solute association in any such system.

References

Abraham, G. N., Podell, D. N., Wistar, R., Johnston, S. L., & Welch, E. H. (1979) *Clin. Exp. Immunol. 36*, 63–70.

Adams, E. T., Jr., & Williams, J. W. (1964) *J. Am. Chem. Soc. 86*, 3454–3461.

Adams, E. T., Jr., & Filmer, D. L. (1966) *Biochemistry 5*, 2971–2985.

Adams, E. T., Tang, L. H., Sarquis, J. L., Barlow, G. H., & Norma, W. M. (1978) in *Physical Aspects of Protein Interactions* (Catsimpoolas, N., Ed.) pp 1–55, Elsevier/North-Holland, Inc., New York.

Asakura, S. (1968) *J. Mol. Biol. 35*, 237–239.

Bjorneboe, M., & Jensen, K. B. (1966) *Acta. Med. Scand., Suppl. No. 445*, 212–215.

Brouet, J. D., Clauvel, J. P., Danon, F., Klein, M., & Seligman, M. (1975) *Am. J. Med. 57*, 775–788.

Bull, H. B., & Breese, K. (1968) *J. Phys. Chem. 72*, 1817–1819.

Chervenka, C. H. (1969) *A Manual of Methods for the Analytical Ultracentrifuge*, Spinco Div., Beckman Instruments, Palo Alto, CA, p 17.

Chun, P. W., Kim, S. J., Williams, J. W., Cope, W. T., Tang, L. H., & Adams, E. T. (1972) *Biopolymers 11*, 197–214.

Desnica, D. (1977) *Biopolymers 18*, 1685–1694.

Erikson, B. W., Gerber-Jensen, B., Wang, A., & Litman, G. W. (1982) *Mol. Immunol. 19* (*3*), 357–365.

Green, R. W. (1973) *Biochemistry 12*, 3225–3231.

Hall, C. G., & Abraham, G. N. (1984) *Arch. Biochem. Biophys. 233*, 330–337.

Jeffrey, P. D., & Coates, J. H. (1966) *Biochemistry 5*, 3820.

Kaliner, S. M., & Kegeles, G. (1955) *J. Phys. Chem. 59*, 592.

Klein, M., Kells, D. L. C., Tinker, D. O., & Dorrington, K. J. (1977) *Biochemistry 16*, 552–560.

Kochwa, S., Smith, E., Brownell, M., & Wasserman, L. R. (1966) *Biochemistry 5*, 277–285.

Kyle, R. A., & Bayrd, E. D. (1976) *Monoclonal Gammapathies* pp 219–222, Charles C Thomas, Springfield, IL.

Lauffer, M. A. (1975) *Mol. Biol. Biochem. Biophys. 20*, 1–264.

Lauffer, M. A., & Shalaby, R. S. (1960) *Arch. Biochem. Biophys. 201*, 224–234.

Lindsley, H., Teller, D., Noonan, B., Peterson, M., & Mannik, M. (1973) *Am. J. Med. 54*, 682–688.

Lowenstein, J. M. (1967) in *Metabolic Pathways* (Greenberg, D. M., Ed.) 3rd ed., pp 146–270, Academic Press, New York.

Middaugh, C. R., & Litman, G. W. (1977a) *FEBS Lett. 79*, 200–202.

Middaugh, C. R., & Litman, G. W. (1977b) *J. Biol. Chem. 252*, 8002–8006.

Middaugh, C. R., Kelloe, J. M., Prystowsky, M. B., Gerber-Jenson, B., Jenson, J. C., & Litman, G. W. (1978) *Immunochemistry 15*, 171–187.

Middaugh, C. R., Tisel, W. A., Haire, R. N., & Rosneberg, A. (1979) *J. Biol. Chem. 254*, 367–370.

Middaugh, C. R., Lawson, E. Q., Litman, G. W., Tisel, W. A., Mood, D. A., & Rosenberg, A. (1980) *J. Biol. Chem. 255*, 6532–6534.

Miekka, S. L., & Litman, G. W. (1978) *Arch. Biochem. Biophys. 191*, 525–536.

Millthorpe, B. K., Jeffrey, P. D., & Nichol, L. W. (1975) *Biophys. Chem. 3*, 169.
Olmsted, J. B., & Borisy, G. G. (1973) *Annu. Rev. Biochem. 42*, 507–540.
Oosawa, F., & Kasai, M. (1971) *Subunits in Biological Systems* (Timasheff, S. N., Ed.) Part A, pp 261–322, Marcel Dekker, New York.
Oosawa, F., & Asakura, S. (1975) *Thermodynamics of the Polymerization of Protein*, Chapter 5, Academic Press, London.
Parker, C. W., & Osterland, C. K. (1970) *Biochemistry 9*, 1074–1082.
Pope, R. M., Mannik, M. M., Gilliland, B. C., & Teller, D. C. (1975) *Arthritis Rheum. 18*, 97–106.
Pruzanski, W., & Watt, J. G. (1972) *Ann. Intern. Med. 77*, 853–860.
Pruzanski, W., & Russel, M. L. (1976) *Am. J. Med. Sci. 271*, 145–150.
Sarquis, J. L., & Adams, E. T., Jr. (1976) *Arch. Biochem. Biophys. 163*, 442.
Scoville, C. D., Abraham, G. N., & Turner, D. H. (1979) *Biochemistry 18*, 2610–2615.
Scoville, C. D., Turner, D. H., Lippert, J. L., & Abraham, G. N. (1980) *J. Biol. Chem. 255*, 5847–5852.
Shalaby, R. A., & Lauffer, M. A. (1980) *Arch. Biochem. Biophys. 204*, 494–502.
Squire, P. G., & Li, C. H. (1961) *J. Am. Chem. Soc. 83*, 3521.
Stevens, C. L., & Lauffer, M. A. (1965) *Biochemistry 4*, 31–37.
Stevens, F. J., Westholm, F. A., Solomon, A., & Schiffer, M. (1980) *Proc. Natl. Acad. Sci. U.S.A. 77*, 1144–1148.
Tang, L. H., Powell, D. R., Escott, B. M., & Adams, E. T., Jr. (1977) *Biophys. Chem. 7*, 121–139.
Timasheff, S. N. (1973) *Protides Biol. Fluids 20*, 511.
Ungewickell, E., & Gratzer, W. (1978) *Eur. J. Biochem. 88*, 379–385.
Vialtel, P., Kells, D. L. C., Pintenc. L., Dorrington, K. J., & Klein, M. (1982) *J. Biol. Chem. 257*, 3811–3818.
Vogel, O., Hoehn, B., & Henning, U. (1972) *Eur. J. Biochem. 30*, 354–360.
White, J. F., & Heagan, B. (1970) *J. Exp. Med. 131*, 1079–1092.
Yphantis, D. A. (1964) *Biochemistry 3*, 297.

Evidence for the Control of the Action of Phospholipases A by the Physical State of the Substrate†

Tom Thuren, Petri Vainio, Jorma A. Virtanen, Pentti Somerharju, Kurt Blomqvist, and Paavo K. J. Kinnunen*

ABSTRACT: Fluorescence and monolayer techniques were used as complementary methods to study the effect of NaCl on (i) the conformation of phosphatidylglycerol present in vesicles or monolayers and on (ii) the activities of phospholipases A on these lipids. The mean molecular area in monolayers of 1,2-didodecanoyl-*sn*-glycero-3-phospho-*rac*-glycerol ($diC_{12}PG$) at an air/water interface was measured and at a surface pressure of 15 dyn cm^{-1} did expand from 63 to 76 Å molecule when the NaCl concentration was increased from 0 to 1.0 M, respectively. Simultaneously with the increase in the salt concentration up to 1.0 M pancreatic phospholipase A_2 (PLA_2) was inhibited by 95% whereas bovine milk lipoprotein lipase here employed as phospholipase A_1 (PLA_1) was activated. No PLA_1 activity could be measured in the absence of NaCl. The electrolyte had no effect on the penetration of these enzymes into a film of a nonhydrolyzable substrate analogue, 1,2-dihexadecyl-*sn*-glycero-3-phospho-*rac*-glycerol (diEPG). The NaCl-induced changes were further examined by using vesicles of 1,2-bis[(pyren-1-yl)butanoyl]-*sn*-glycero-3-phospho-*rac*-glycerol (diPBPG). The ratio of pyrene excimer to monomer fluorescence intensities (I_e/I_m) increased from 2.9 to 3.3 as the NaCl concentration was increased from 0 to 0.5 M. Hydrolysis of diPBPG by PLA_1 was enhanced by salt 2-fold whereas the activity of PLA_2 was inhibited by 90%. The salt-induced conformational changes in phosphatidylglycerol could be connected with the altered accessibilities of *sn*-1 and *sn*-2 ester bonds to enzymatic hydrolysis. Briefly, it can be assumed that phosphatidylglycerol at low ionic strength is in the so-called "kinked" conformation, the glycerol backbone extending parallel to the *sn*-1 acyl chain, whereas the *sn*-2 chain starts in its first methylene segments parallel to the surface and then bends to align the *sn*-1 chain. At high ionic strength the glycerol backbone should be parallel to the plane of the interface with both acyl chains starting perpendicular to the surface. In the latter conformation an increased molecular surface area for $diC_{12}PG$ monolayer is observed. In spite of the predicted salt-induced increased average spacing between the phospholipids, an enhanced rate of pyrene excimer formation in diPBPG vesicles is evident. The measured salt-induced increase in I_e/I_m of diPBPG is likely to be due to intramolecular excimer formation, thus reflecting the parallel and equal alignment of the (pyren-1-yl)butanoyl chains.

Phospholipases A_1 and A_2 (PLA_1 and PLA_2)[1] hydrolyze respectively the *sn*-1 and *sn*-2 fatty acyl ester bonds of the naturally occurring *sn*-3 phospholipids (de Haas, 1968). These enzymes are found in mammalian both extracellularly serving

† From the Department of Medical Chemistry, University of Helsinki, SF-00170 Helsinki 17, Finland. *Received November 7, 1983.* The results of this study were presented in a lecture delivered by P.K.J.K. during The Enrico Fermi Summer School on Physics of Amphiphiles, Micelles and Microemulsions, held in Varenna, Italy, July 19–29, 1983. This study was supported by Ida Montin Foundation and Yrjö-Jahnsson Foundation (T.T.) and by Finnish Cultural Foundation (P.V.). Major financial support was provided by the Finnish State Medical Council (P.K.J.K.).

[1] Abbreviations: $diC_{12}PG$, 1,2-didodecanoyl-*sn*-glycero-3-phospho-*rac*-glycerol; diEPG, 1,2-dihexadecyl-*sn*-glycero-3-phospho-*rac*-glycerol; diPBPG, 1,2-bis[(pyren-1-yl)butanoyl]-*sn*-glycero-3-phospho-*rac*-glycerol; cmc, critical micellar concentration; ffa, free fatty acid; I_e, pyrene excimer emission intensity; I_m, pyrene monomer emission intensity; PLA, phospholipase A; PLA_1, phospholipase A_1; PLA_2, phospholipase A_2; Tris-HCl, tris(hydroxymethyl)aminomethane hydrochloride; EDTA, ethylenediaminetetraacetic acid.

0006-2960/84/0423-5129$01.50/0